IEEE Access
Multidisciplinary : Rapid Review : Open Access Journal

Received April 2, 2019, accepted May 1, 2019, date of publication May 9, 2019, date of current version May 23, 2019.

Digital Object Identifier 10.1109/ACCESS.2019.2915960

Multi-Beam Metasurface Antenna by Combining Phase Gradients and Coding Sequences

HE WANG[1], YONGFENG LI[1], HONGYA CHEN[1], YAJUAN HAN[1,2], SAI SUI[1], YA FAN[1], ZETIAN YANG[1], JIAFU WANG[1], JIEQIU ZHANG[1], SHAOBO QU[1], AND QIANG CHENG[3]

[1]College of Science, Air Force Engineering University, Xi'an 710051, China
[2]School of Physics and Optoelectronic Engineering, Xidian University, Xi'an 710051, China
[3]State Key Laboratory of Millimeter Waves, Southeast University, Nanjing 210096, China

Corresponding authors: Yongfeng Li (liyf217130@126.com) and Shaobo Qu (qushaobo@mail.xjtu.edu.cn)

This work was supported by the National Natural Science Foundation of China under Grant 61331005, Grant 61501503, Grant 61471388, and Grant 61601507. *(He Wang and Hongya Chen contributed equally to this work.)*

ABSTRACT In this paper, we propose a strategy to achieve a single-feed multi-beam metasurface antenna by combining phase gradient and coding sequence. Theoretically, the multi-beam antennas with various far-field patterns can be realized via superimposing different kinds of phase coding sequences. As three proof-of-concepts, the 0101.../0101... coding sequence, chessboard coding sequence, and 1-bit sector coding sequence are selected to design double-beam, four-beam, and eight-beam circular-polarized reflector antennas, respectively. Furthermore, the four-beam reflector antenna is fabricated and measured to demonstrate the feasibility of our strategy. The fabricated antenna can produce four perfect pencil-shaped beams in a wide frequency range from 11 to 13 GHz. At central frequency, the realized gain is about 19.9 dB and the axial ratio is lower than 3 dB. Moreover, the circular polarization state of the reflective beams is consistent with the polarization state of spot source, which differs from the reflector antennas based on the polarization-insensitive unit cells. This paper connects the multi-beam patterns with binary digits, which provide the potential for reconfiguring the multi-beam patterns by computer programs.

INDEX TERMS Metasurfaces, phase gradient, coding sequence, reflector antennas, Pancharatnam-Berry phase.

I. INTRODUCTION

Metasurfaces, as the 2D version of metamaterials, have continuously attracted enormous interest due to their unusual electromagnetic (EM) properties [1]–[13]. They can tailor magnitude and phase of EM waves by controlling periodic unit cells in a sub-wavelength scale [1], [2]. In addition, compared with metamaterials, metasurfaces possess the advantages of low-profile, light-weight and efficient control of aperture field [3]–[6]. Since Capasso's group proposed the generalized laws of refraction/reflection in 2011, many exceptional phenomena and novel devices have been realized [1]–[10], typically in the field of antennas and antenna accessories [11]–[13].

Multi-beam antennas have attracted much attention of researchers due to their practical value in communication applications and radar systems [14]. Recent years, a number of metasurface-based multi-beam antennas have appeared. Ref. [15] has designed single-source and multi-source feeding multi-beam antennas by using a single metasurface aperture divided in several angular sectors or shared by a superposition of individual modulations. Li *et al.* have presented a combined theory of holography and leaky wave to realize the multi-beam radiations by exciting the surface interference patterns, which are generated by interference between the excitation source and required radiation waves [16]. As the frequency changes, we show that the main lobes of EM radiation beams could accomplish 1-D or 2-D scans regularly by using the proposed holographic metasurfaces shaped with different interference patterns. On the same principle, a three-beam dual-Polarization printed holographic multi-beam metasurface antenna is demonstrated numerically and experimentally [17]. Fortunately, these articles paved a new route to eliminating the complicated steps of using the Fourier transform to deduce the required amplitude and phase of conventional antenna arrays.

In 2014, Tiejun Cui *et al.* proposed the concept of coding metasurfaces (CMs), which delivered a connection

The associate editor coordinating the review of this manuscript and approving it for publication was Muhammad Zubair.

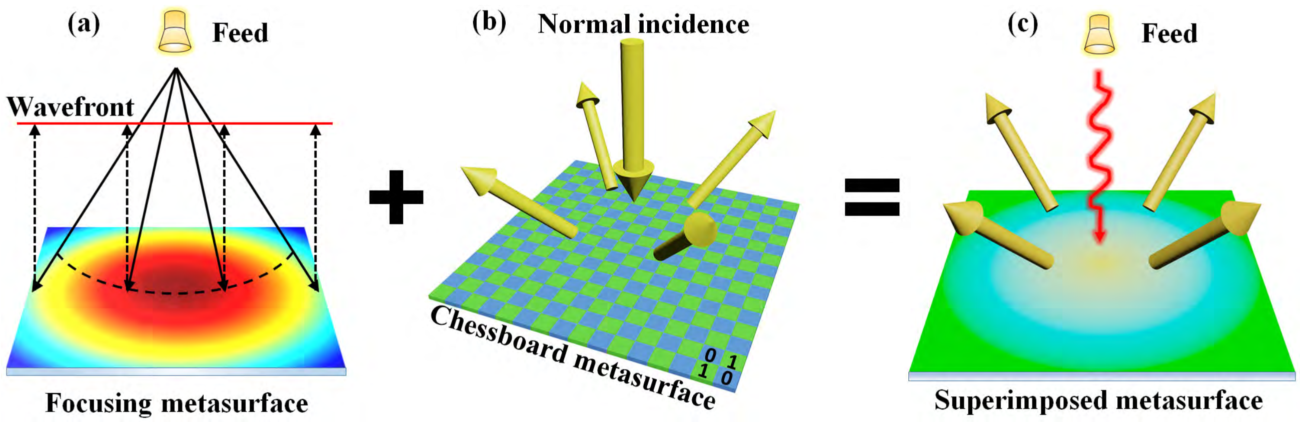

FIGURE 1. Design principle of multi-beam metasurface reflector antennas: (a) PGM with parabolic spatial phase distribution, (b) CM with chessboard coding sequence, (c) metasurface with superimposed phase distribution.

between the physical metasurface unit cells and digital codes [18]. Unit cells of them, known as "metamaterial bits" with binary codes "0" and "1", can be realized by phases 0° and 180° [19]. Accordingly, binary digital information can be directly encoded on the metasurfaces which provides a more flexible and efficient way to manipulate EM waves [20]. By arranging the coding elements in a 2D plane with the predesigned coding sequence, many unique functionalities can be achieved, including anomalous refraction/reflection [21]–[22], broadband diffusions [23], multi-functional metasurfaces [24], and beamforming [25], etc. Particularly, CMs can be used for beam splitting, so they have great potentials in designing multi-beam devices. Unfortunately, it is rarely reported that the design of multi-beam antennas combined the mechanisms of CMs.

In this paper, we proposed a selective strategy to achieve multi-beam antenna by integrating phase gradient metasurface (PGMs) and CMs. Theoretically, the strategy can be used to achieve arbitrary multi-beam patterns through varying the coding sequence. As three design examples, we numerically demonstrate double-beam, four-beam and eight-beam circular-polarized reflector antennas by combining focusing metasurface and CMs, and experimentally verify the feasibility of four-beam reflector antenna. In our design, a Z-shaped circular polarization sensitive unit cell based on Pancharatnum-Berry (PB) phase is proposed to assemble the metasurface reflector to achieve high efficient co-polarization reflection. The advantage of this work is that it simplifies the design of multi-beam metasurface antennas. Moreover, this work connects the multi-beam patterns with binary digits which provide the potential for reconfiguring the multi-beam patterns by computer programs. To the best of our knowledge, it is the first time to propose such a strategy, which may have promising significance for simultaneous multi-directional transmitting/receiving antennas and beam reconfigurable antennas in applications of radar and communication systems.

II. DESIGN PRINCIPLE

The principle of realizing multi-beam radiation is to introduce plane wave front by focusing metasurface and then split it into multiple directions by coding sequence. When a spot source irradiates on the reflector surface, the phase of reflected waves will be non-uniform because of the different transmitting path lengths in free space as shown in Fig.1 (a). To realize planar reflection, PGM with parabolic spatial phase distribution is imposed to remove the phase difference, which the phase profile governed by:

$$\varphi(x, y) = \varphi_0 + \frac{2\pi}{\lambda}\left(\sqrt{x^2 + y^2 + F^2} - F\right) \tag{1}$$

where φ_0 is the reflected phase of the unit cell located at the origin position, λ is the operating wavelength in free space, and F is focal length.

CMs are a special kind of metasurfaces which use binary codes to represent phase. Considering a general CM consists of $N \times N$ array of coded elements, and each element composed of $M \times M$ unit cells. Since the reflection coefficient of each coding unit cell is equal, the CM can be considered as a passive antenna array. Therefore, when the plane EM illuminated perpendicularly, the far-field function can be expressed as:

$$F(\theta, \varphi) = f_{m,n}(\theta, \varphi) S_a(\theta, \varphi) \tag{2}$$

where θ and φ are the elevation and azimuth angles of the rejected wave, $f_{m,n}(\theta, \varphi)$ represents the primary pattern that can regulate the vector parameters of far-field such as polarization and directional pattern. $S_a(\theta, \varphi)$ is the array pattern which is a scalar quantity, and it can be further expressed as:

$$\begin{aligned} S_a(\theta, \varphi) = \sum_{m=1}^{N}\sum_{n=1}^{N} \exp\{j\,[\varphi_{m,n} + k_0 D_x (m - 1/2) \\ \times (\sin\theta\cos\varphi - \sin\theta_i\cos\varphi_i) \\ + K_0 D_y (n - 1/2)(\sin\theta\sin\varphi - \sin\theta_i\sin\varphi_i)]\} \end{aligned} \tag{3}$$

where k_0 is the wave vector, $\varphi_{m,n}$ is the reflection phase of each coding element, D_x and D_y are the size of the coding element in x direction and y direction, θ_i and φ_i are the elevation and azimuth angles of the incident wave, respectively. Fig.1 (b) depicts the chessboard metasurface as the conceptual example, where the blue squares represent "0", and the green squares represent "1". When the plane EM waves impinge on the chessboard metasurface, four equal sized beams can be achieved.

By superimposing parabolic spatial phase distribution and coding sequence, the metasurface reflector simultaneously possesses the function of shaping wave-front and splitting waves. Fig.1 (c) illustrates the schematic of combining CMs and PGMs. When a source feed illuminates on it, it can acquire distinct four beams theoretically, which will have better directional than chessboard metasurface under plane wave normal incidence.

III. DESIGN AND ANALYSIS

A. DESIGN OF THE UNIT CELLS

In this paper, a Z-shaped unit cell [26] is proposed to realize the circularly polarization-keeping. This unit cell consists of a Z-shaped metal structure patterned on a copper-grounded F4B substrate ($\varepsilon_r = 2.65$, $tan\ \delta = 0.001$). Optimizing by CST Studio, the structure parameters are fixed as shown in the inset of the Fig.2 (c), where $a = 6.5$ mm, $b = 4.9$ mm, $d = 3$ mm and $l = 3.5$ mm. The yellow Z-shaped metallic pattern represents the initial state of the unit cell, where $\gamma = 0°$.

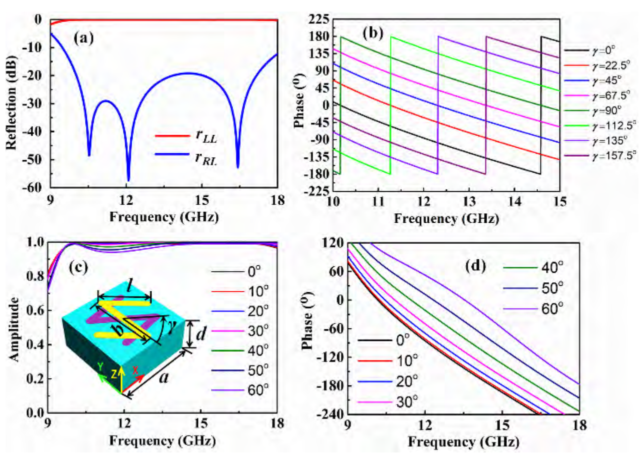

FIGURE 2. Simulated performance of the Z-shaped unit cell: (a) Co- and cross-polarization reflection under normal LHCP wave incidence, (b) phase in different rotation angle γ of Z-shaped metal structure, (c) amplitude of Z-shaped unit cell in different incident angle of EM waves, (d) Phase in different incident angle of EM waves.

The simulated co- and cross-polarization reflection coefficients are given in Fig. 2(a), where r_{LL} is the co-polarization reflection coefficient under the incidence of left-handed circular-polarized (LHCP) waves and r_{RL} is the cross-polarized one. It is observed that the co-polarization reflection carries about 98% energy of incidence, and the cross-polarization reflection carries about 2%. Because of the design of the Z-shaped unit cell is based on Pancharatnam-Berry phase, the phase shift and rotation angle following the expression: $\Delta\Phi = 2\gamma$, where γ is rotation angle. Fig.2 (b) illustrates the phase responses of the Z-shaped unit cell with a different rotation angle. As γincreasing from 0° to 157.5° with step angle 22.5° from 10 GHz to 15 GHz, the phase interval of each curve is 45° which manifests that the unit cell satisfies the design requirement. Fig.2 (c) and (d) show the co-polarized reflection amplitude and phase of the Z-shaped unit cell under different incident angles. *Xoy*-plane is the reference plane of the oblique incidence, and $\gamma = 0°$. It is evident that the amplitude is larger than 0.9 from 10 GHz to 18 GHz when the incident angle increases from 0° to 60°. As the incident angle is less than 10°, the phase response is almost constant at the same frequency. But when the incident angle increases to more than 20°, the phase response changes dramatically. To decrease the impact of the incident angle, it is necessary to discretize incident angle and compensate for the delay of the phase response. According to the simulated results of proposed unit cell, we define the initial state of the unit cell is coded digit "0", and the counterpart of $\gamma = 90°$ is "1". Fig.3 shows the schematics of defined coded digits and the corresponding reflection amplitude and phase. As can be seen, the amplitudes of different coded digits are nearly identical. Besides, the phase difference is 180° in 10-18 GHz.

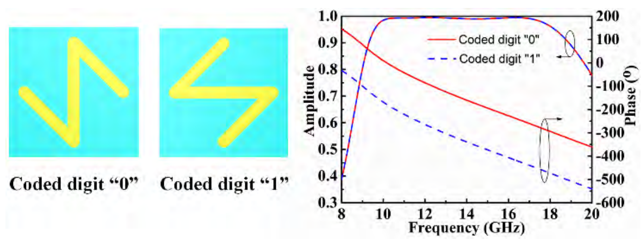

FIGURE 3. Pictures of defined coded digits "0" and "1" with the corresponding results of reflection amplitude and phase.

B. DESIGN PROCEDURES OF THE MULTI-BEAM REFLECTOR ANTENNA

The designing process of the multi-beam reflector antenna can be divided into three steps:

Firstly, we designed a planar reflector antenna which consists of a metasurface reflector and a helical antenna. The reflector is assembled by Z-shaped unit cells with the different rotation angle calculated via Equation (1). The radius of the metasurface is 156 mm and the thickness is 3mm. To guarantee at least half of the power of the helical antenna impinging on reflective metasurface, the half-power bandwidth (HPBW) of the helical antenna is designed as same as the opening angle of the helical antenna to the edge of the metasurface (in here is 32°). Considering the influence of phase delay delivered by the different incident angle of EM wave (which has a greater impact on the position and depth of

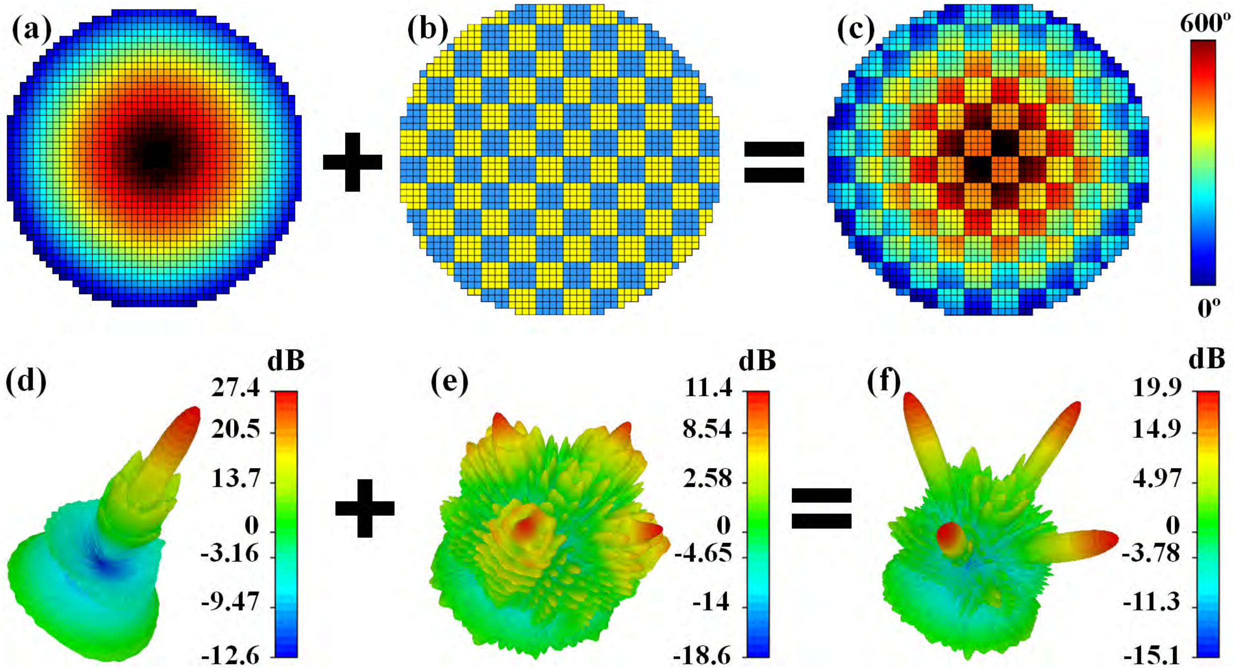

FIGURE 4. Phase distribution and simulated far-field radiation pattern of: (a), (d) focusing metasurface; (b), (e) chessboard metasurface; (c), (f) superposition metasurface, respectively.

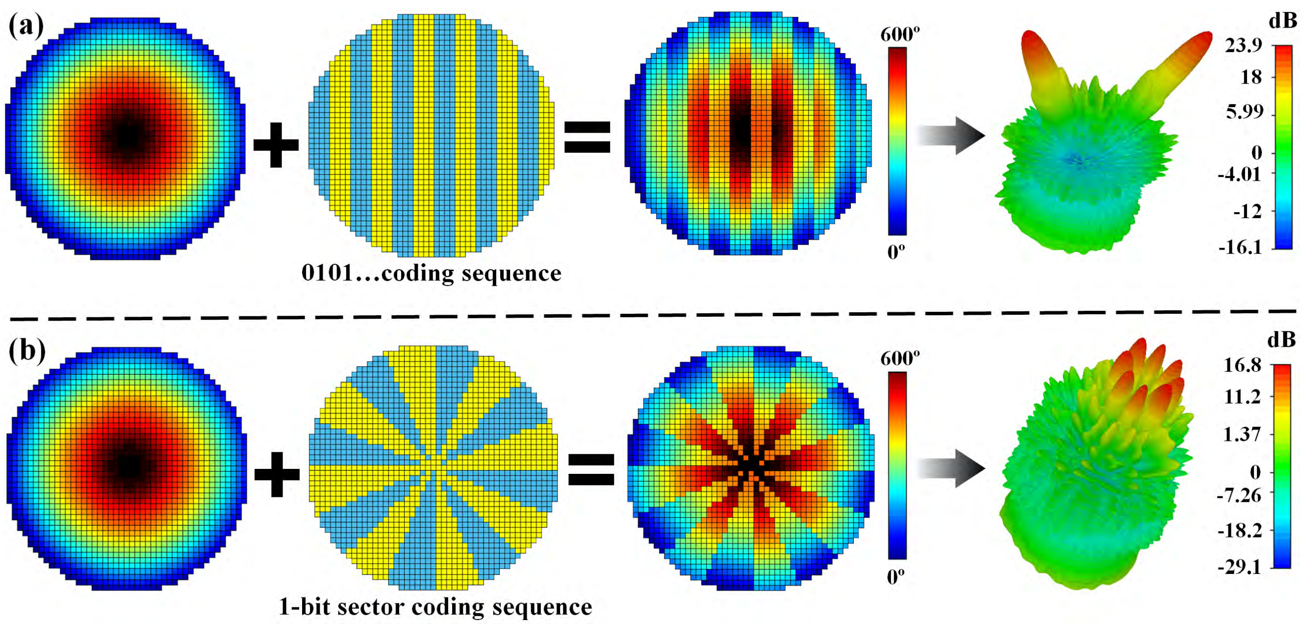

FIGURE 5. Phase distribution and simulated far-field radiation pattern of: (a) double-beam metasurface reflector antenna, (b) eight-beam metasurface reflector antenna.

the focal point), we discretize the value of incident angle and compensate the phase delay according to fluctuation in phase response as shown in Fig.2(d). The method of discretization and compensation is shown in TABLE 1. Here, we compensated for the phase by 5^{o} according to the incident angle. The helical antenna is placed above the reflective metasurface with the distance of 250 mm to the center. Fig.4 (a) illustrates the phase distribution of the reflector, and Fig.4 (d) presents the simulated far-field pattern at 12 GHz. It is observed that a single narrow pencil-shaped beam is obtained, and the realized gain is 27.4 dB.

Secondly, we designed a reflective coding metasurface with the same size of the aforementioned focusing metasurface, and the feed is placed in the same position.

TABLE 1. Angle compensation.

Number	1	2	3	4	5	6	7
Discretized incident Angle	0°-10°	10°-15°	15°-21°	21°-25°	25°-28°	28°-30°	30°-32°
Compensated Phase	0°	5°	10°	15°	20°	25°	30°

As an example, chessboard coding sequence is selected and depicted in Fig.4 (b), the phase distribution is crossed by "0" and "1" as 0101... /1010... When the chessboard metasurface is illuminated by helical feeding antenna at 12 GHz, the far-field radiation pattern is shown in Fig.4 (e). The far-field radiation pattern shows four ambiguous beams with huge side lobes, which manifests that the energy is not concentrated. Besides, the realized gain is lower with 11.4 dB at 12 GHz.

Thirdly, we superimposed the phase distributions of focusing metasurface and chessboard metasurface. Accordingly, the plane wave is perfectly split into four beams. The superimposed phase distribution is depicted in Fig.4 (c), and the far-field pattern is shown in Fig.4 (f). Four distinct pencil-shaped beams are obtained with the gain of 19.9 dB at 12 GHz, which is about a quarter of the gain of the planar reflector antenna 27.4 dB presented in Fig.4 (d). Because the beam is divided into four equal one, the energy should be one quarter of the planar reflector antenna (the gain should be reduced by 6 dB).

In order to further prove the effectivity of our strategy, we use the same approaches to superimpose 0101.../0101...coding sequence and 1-bit sector coding sequence to achieve double-beam and eight-beam antennas, respectively. The coding sequences and the corresponding simulated far-field patterns are illustrated in Fig. 5 (a) and (b), which manifest that the distinct double-beam pattern and eight beam pattern can be attained successfully with realized gain of 23.9 dB (approximately half of 27.4 dB) and 16.8 dB (approximately 1/8 of 27.4 dB) at 12 GHz, respectively. Moreover, many other coding sequences can be selected to achieve different far-field patterns, which are not listed in this paper for brevity.

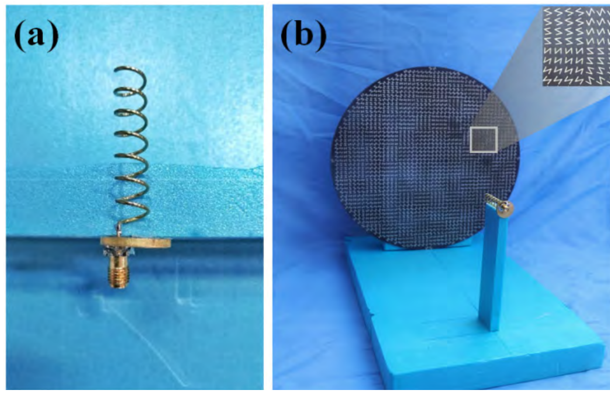

FIGURE 6. Photographs of the fabricated samples: (a) feed helical antenna, (b) multi-beam planar reflector antenna.

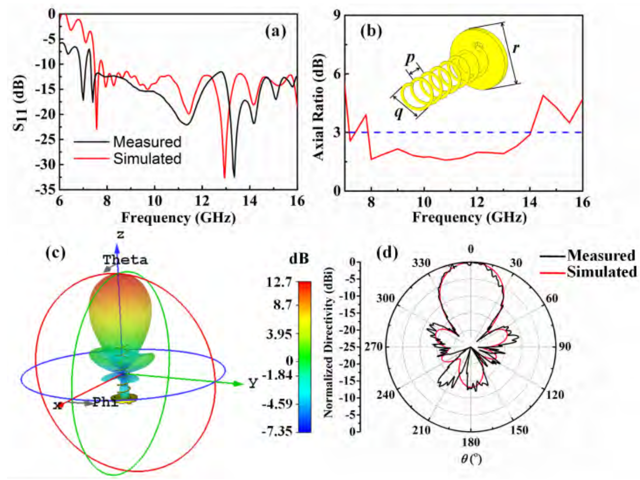

FIGURE 7. Performance of the feed helical antenna: (a) S_{11}, (b) axial ratio bandwidth with inset of helical antenna, (c) simulated 3-D far-field pattern at 12 GHz, (d) normalized directivity at 12 GHz ($\varphi = 90°$).

IV. SIMULATIONS AND EXPERIMENTS

To experimentally verify the method, we selected four-beam metasurface reflector antenna for fabrication and carried out the experiments in an anechoic chamber to reduce the environment interference. In the experiment, the designed antenna works as transmitter and a standard horn antenna as receiver. Fig.6 (a) and (b) present the photographs of feed helical antenna and multi-beam planar reflector antenna of which helical antenna and reflector are respectively fixed on two foams with distance of 250 mm.

A. HELICAL ANTENNA

At first, the performances of helical antenna was simulated and measured. The structure of the helical antenna is shown in the inset of Fig.7 (b), where $p = 5.7$ mm, $q = 10$ mm, $r = 20$ mm. Fig.7 (a) illustrates the simulated and measured S_{11}. It is observed that the measured curve is in good accordance with the simulated one, except for a slight blue shift. Both the curves manifest that the feed helical antenna with good impedance match from 8 to 16 GHz. Fig.7 (b) shows the axial ratio bandwidth. Axial ratio in the main lobe direction is less than 3 dB over 8-14 GHz which indicates that the radiation beam is circularly polarized. Simulated 3-D far-field radiation pattern of the helical antenna is shown in Fig.7 (c). The realized gain is 12.7 dB in the maximum direction at 12GHz. Moreover, the simulated and measured curves of normalized directivity in the cutting plane of $\varphi = 90°$ are

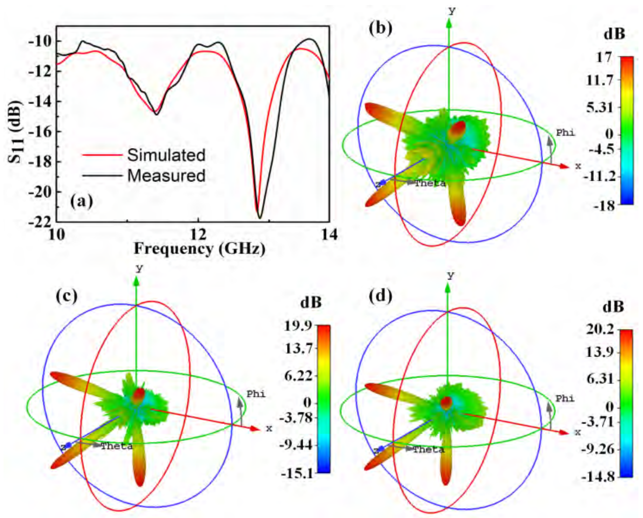

FIGURE 8. (a) S_{11} of the designed multi-beam planar reflector antenna. Simulated 3-D far-field radiation patterns at: (b) 11 GHz, (c) 12 GHz and (d) 13 GHz.

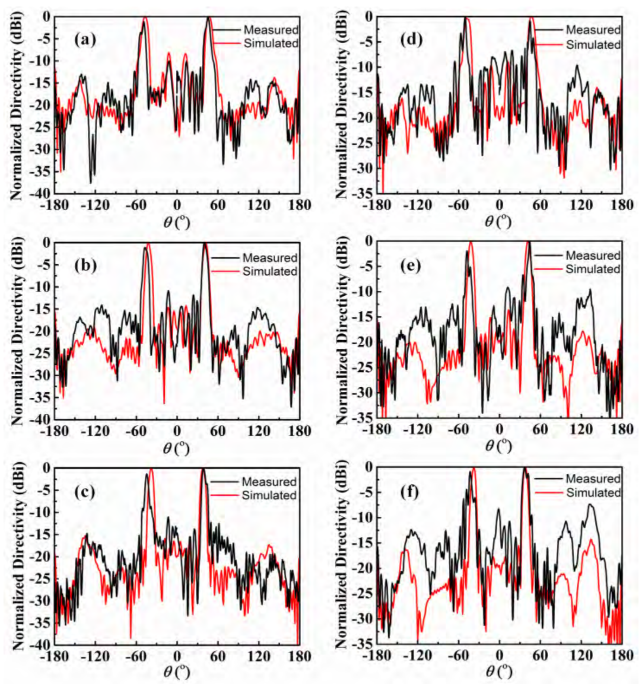

FIGURE 9. The simulated and measured normalized directivity of designed multi-beam reflector antenna: (a) $\varphi = 45°$, 11 GHz, (b) $\varphi = 45°$, 12 GHz, (c) $\varphi = 45°$, 13 GHz, (d) $\varphi = 135°$, 11 GHz, (e) $\varphi = 135°$, 12 GHz, (f) $\varphi = 135°$, 13 GHz.

presented in Fig.7 (d). The above results manifest that the helical antenna is suitable as a spot source. The slight disparity between the measured and simulated results is due to the inaccuracies in welding of helical antenna and the uncertainty in the measure environment.

B. MULTI-BEAM PLANAR REFLECTOR ANTENNA

By fixing the helical antenna at the focal point of metasurface reflector, the performance of the four-beam reflector antenna is presented as follow. The S_{11} of the multi-beam planar reflector is depicted in Fig.8 (a). Both the measured and simulated curves are below than -10 dB from 11 GHz to 13 GHz. Fig.8 (b)-(d) depict the simulated 3-D far-field patterns of the multi-beam planar reflector antenna at 11 GHz, 12 GHz and 13 GHz with the realized gain 17 dB, 19.9 dB and 20.2 dB, respectively.

Moreover, the far-field patterns of the designed antenna in cutting planes $\varphi = 45°$ and $\varphi = 135°$ were simulated and measured at 11GHz, 12GHz and 13GHz as shown in Fig.9, respectively. Both the simulated and measured results present that the designed multi-beam planar reflector antenna can get four equally distinct pencil-shaped beams in 11-13 GHz. It is observed that the measured curves are in good accordance with simulated curves. The slight deviation in the main-lobe direction between the measurements and simulations is due to the unavoidable tilt of the helical antenna during the experiment. In a word, the results demonstrate the proposed strategy is feasible to design multi-beam reflector antennas. In addition, the four-beam antenna may have the potential to apply as a detecting antenna.

V. CONCLUSION

In this paper, we proposed and verified the strategy of combining PGMs and CMs to design single-feed multi-beam metasurface reflector antennas. For verification, double-beam, four-beam and eight-beam reflector antennas is designed and simulated by CST studio. Especially, we fabricated the four-beam reflector antenna and carried out the experiments to demonstrate the feasibility. The fabricated antenna can work from 11 GHz to 13 GHz with four high gain pencil-shaped beams. At the central frequency, the realized gain of designed antenna is 19.9 dB. Importantly, this strategy provides a new idea of designing multi-beam antennas by integrating computer to control the coding sequence, which let the design of multi-beam antennas more flexible and has significance in communication applications.

REFERENCES

[1] N. F. Yu *et al.*, "Light propagation with phase discontinuities: Generalized laws of reflection and refraction," *Science*, vol. 334, pp. 333–337, Oct. 2011.

[2] F. Aieta *et al.*, "Reflection and refraction of light from metasurfaces with phase discontinuities," *Proc. SPIE*, vol. 6, no. 1, pp. 063532-1–063532-9, Dec. 2012.

[3] K. Yao and Y. Liu, "Plasmonic metamaterials," *Nanotechnol. Rev.*, vol. 3, no. 2, pp. 177–210, Jan. 2014.

[4] L. Cui *et al.*, "Polarization-dependent bi-functional metasurface for directive radiation and diffusion-like scattering," *AIP Adv.*, vol. 7, no. 11, Nov. 2017, Art. no. 115214.

[5] N. Yu and F. Capasso, "Flat optics with designer metasurfaces," *Nature Mater.*, vol. 13, pp. 139–150, Jan. 2014.

[6] L. Liu *et al.*, "Broadband metasurfaces with simultaneous control of phase and amplitude," *Adv. Mater.*, vol. 26, no. 29, pp. 5031–5036, Aug. 2014.

[7] H. L. Zhu, S. W. Cheung, K. L. Chung, and T. I. Yuk, "Linear-to-circular polarization conversion using metasurface," *IEEE Trans. Antennas Propag.*, vol. 61, no. 9, pp. 4615–4623, Sep. 2013.

[8] O. Eisenbach, O. Avayu, R. Ditcovski, and T. Ellenbogen, "Metasurfaces based dual wavelength diffractive lenses," *Opt. Express*, vol. 23, no. 4, pp. 3928–3936, 2015.

[9] P. Su, Y. Zhao, S. Jia, W. Shi, and H. Wang, "An ultra-wideband and polarization-independent metasurface for RCS reduction," *Sci. Rep.*, vol. 6, Feb. 2016, Art. no. 20387.

[10] M. Uchida and A. Tonomura, "Generation of electron beams carrying orbital angular momentum," *Nature*, vol. 464, pp. 737–739, Apr. 2010.

[11] D. Ramaccia, F. Scattone, F. Bilotti, and A. Toscano, "Broadband compact horn antennas by using EPS-ENZ metamaterial lens," *IEEE Trans. Antennas Propag.*, vol. 61, no. 6, pp. 2929–2937, Jun. 2013.

[12] S. M. Chaker and M. Bouzouad, "Metamaterial patch antenna radiation pattern agility," *Appl. Phys. A, Solids Surf.*, vol. 115, no. 2, pp. 459–465, 2014.

[13] D. Ramaccia *et al.*, "Exploiting intrinsic dispersion of metamaterials for designing broadband aperture antennas: Theory and experimental verification," *IEEE Trans. Antennas Propag.*, vol. 64, no. 3, pp. 1141–1146, Mar. 2016.

[14] Y. Han *et al.*, "Multibeam antennas based on spoof surface plasmon polaritons mode coupling," *IEEE Trans. Antennas Propag.*, vol. 65, no. 3, pp. 1187–1192, Mar. 2017.

[15] D. González-Ovejero, G. Minatti, G. Chattopadhyay, and S. Maci, "Multibeam by metasurface antennas," *IEEE Trans. Antennas Propag.*, vol. 65, no. 6, pp. 2923–2930, Jun. 2017.

[16] Y. B. Li, X. Wan, B. G. Cai, Q. Cheng, and T. J. Cui, "Frequency-controls of electromagnetic multi-beam scanning by metasurfaces," *Sci. Rep.*, vol. 4, Nov. 2014, Art. no. 6921.

[17] O. Yurduseven and D. R. Smith, "Dual-polarization printed holographic multibeam metasurface antenna," *IEEE Antennas Wireless Propag. Lett.*, vol. 16, pp. 2738–2741, 2017.

[18] T. Cui, M. Q. Qi, X. Wan, J. Zhao, and Q. Cheng, "Coding metamaterials, digital metamaterials and programmable metamaterials," *Light, Sci. Appl.*, vol. 3, p. e218, Oct. 2014.

[19] Z. Shen *et al.*, "Design of transmission-type coding metasurface and its application of beam forming," *Appl. Phys. Lett.*, vol. 109, no. 12, 2016, Art. no. 121103.

[20] L. Zhang *et al.*, "Transmission-reflection-integrated multifunctional coding metasurface for full-space controls of electromagnetic waves," *Adv. Funct. Mater.*, vol. 28, no. 33, Aug. 2018, Art. no. 1802205.

[21] S. Liu *et al.*, "Anisotropic coding metamaterials and their powerful manipulation of differently polarized terahertz waves," *Light, Sci. Appl.*, vol. 5, May 2016, Art. no. e16076.

[22] S. Liu *et al.*, "Anomalous refraction and nondiffractive bessel-beam generation of terahertz waves through transmission-type coding metasurfaces," *ACS Photon.*, vol. 3, no. 10, pp. 1968–1977, Sep. 2016.

[23] L. H. Gao *et al.*, "Broadband diffusion of terahertz waves by multi-bit coding metasurface," *Light, Sci. Appl.*, vol. 4, p. e324, Sep. 2015.

[24] S. Liu *et al.*, "Frequency-dependent dual-functional coding metasurfaces at terahertz frequencies," *Adv. Opt. Mater.*, vol. 4, pp. 1965–1973, Dec. 2016.

[25] C. Huang, B. Sun, W. Pan, J. Cui, X. Wu, and X. Luo, "Dynamical beam manipulation based on 2-bit digitally-controlled coding metasurface," *Sci. Rep.*, vol. 7, Feb. 2017, Art. no. 42302.

[26] L. Yong-Feng *et al.*, "Wide-band circular polarization-keeping reflection mediated by metasurface," *Chin. Phys. B*, vol. 24, no. 1, 2015, Art. no. 014202.

HE WANG received the B.E. degree in communication engineering from Air Force Engineering University, Xi'an, Shaanxi, China, in 2017, where he is currently pursuing the master's degree in physical electronics. His research interests include metasurfaces and antennas design.

YONGFENG LI received the B.S., M.S., and Ph.D. degrees in physical electronics from Air Force Engineering University, Xi'an, Shaanxi, China, in 2008, 2010, and 2015, respectively. He has been with Air Force Engineering University, since 2015. His research interests include the surface wave, phase gradient metasurfaces, code metasurfaces, and spoof surface plasmon polaritons.

HONGYA CHEN received the B.S. degree in physics from National Defense Science and Technology University, Changsha, China, in 2006, the M.S. degree in optics engineering, and the Ph.D. degree in physical electronics from Air Force Engineering University, Xi'an, China, in 2009 and 2017, respectively. Since 2007, she has been with Air Force Engineering University, where she is currently a Lecturer of physic electronics. Her current research interests include polarized metasurface, spoof surface plasmon polaritons, and the design of metamaterials.

YAJUAN HAN received the B.E. degree in electrical engineering and automation from the Hefei University of Technology, Hefei, Anhui, China, in 2012, and the B.S. degree in electronic science and technique from Air Force Engineering University, Xi'an, China, in 2017. She is currently pursuing the Ph.D. degree with the School of Physics and Optoelectronic Engineering, Xidian University. Her research interests include metasurfaces, spoof surface plasmon polaritons, and antenna design based on metasurface and spoof surface plasmon polaritons.

SAI SUI received the B.S. degree in computer science and technology and the M.S. degree in physical electronics from Air Force Engineering University, Xi'an, Shaanxi, China, in 2013 and 2016, respectively, where he is currently a Lecturer with the College of Science. His research interests include metasurfaces, optimization, frequency selective surfaces, metamaterials, metasurfaces, and absorbers.

YA FAN received the B.S. and M.S. degrees in physical electronics from Air Force Engineering University, Xi'an, China, in 2013 and 2015, respectively, where he is currently pursuing the Ph.D. degree in physical electronics. His current research interests include surface plasmon polaritons, design of metasurfaces, and the application of metasurfaces in microwave devices.

ZETIAN YANG received the B.E. degree in electrical engineering and automation from Air Force Engineering University, in 2017, where he is currently pursuing the Ph.D. degree with the Department of Basic Sciences. His research interests include metasurfaces, piezoelectrics, ferroelectrics, and their applications.

JIAFU WANG received the B.S. degree in radar engineering, the M.S. degree in optics engineering, and the Ph.D. degree in physical electronics from Air Force Engineering University, Xi'an, Shaanxi, China, in 2004, 2007, and 2010, respectively. He has been with Air Force Engineering University, since 2011, where he is currently an Associate Professor in physical electronics. His current research interests include plasma stealth, design of metamaterials, and application of the metamaterials in microwave devices.

JIEQIU ZHANG received the B.S. degree in physics from Navy Engineering University, Wuhan, China, in 1980, the M.S. and Ph.D. degrees in radio physics and electronics from Xi'an Electronic and Technology University, Xi'an, China, in 1992 and 2004, respectively. Since 2001, he has been with the Department of Applied Mathematics and Physics, Air Force Engineering University, Xi'an, China, where he is currently a Professor in physical electronics. His research interests include the theory and application of metamaterials, surface plasma polaritons, and the design of antennas and radar stealth.

SHAOBO QU received the B.S. degree in physics from Fuyang Normal College, Fuyang, Anhui, China, in 1984, the M.S. degree in physics from Sichuan Normal University, Chengdu, China, in 1991, and the Ph.D. degree in materials science and engineering from Northwest Polytechnical University, Xi'an, China, in 2001. Since 2001, he has been with the Department of Applied Mathematics and Physics, Air Force Engineering University, Xi'an, where he is currently a Professor in physical electronics. His research interests include materials physics, metamaterials, electronic materials, and devices.

QIANG CHENG received the Ph.D. degree in electrical engineering from Southeast University, Nanjing, China, in 2008. He joined the Department of Radio Engineering, Southeast University, where he is currently a Full Professor. His research interests include engineered electromagnetic structures, metamaterials, electromagnetic band-gap materials, frequency-selective surfaces, microwave imaging, and millimeter/terahertz circuits.